Three-Dimensional Printing: Basic Principles and Applications in Medicine and Radiology

Guk Bae Kim, PhD[1], Sangwook Lee, BS[1], Haekang Kim, BS[1], Dong Hyun Yang, MD, PhD[2], Young-Hak Kim, MD, PhD[3], Yoon Soo Kyung, MD, PhD[4], Choung-Soo Kim, MD, PhD[5], Se Hoon Choi, MD, PhD[6], Bum Joon Kim, MD[7], Hojin Ha, PhD[8], Sun U. Kwon, MD, PhD[7], Namkug Kim, PhD[9]

[1]Biomedical Engineering Research Center, Asan Institute of Life Science, Asan Medical Center, Seoul 05505, Korea; Departments of [2]Radiology, [3]Cardiology, [4]Health Screening and Promotion Center, [5]Urology, [6]Thoracic and Cardiovascular Surgery, [7]Neurology, and [9]Convergence Medicine, Asan Medical Center, University of Ulsan College of Medicine, Seoul 05505, Korea; [8]POSTECH Biotech Center, Pohang University of Science and Technology, Pohang 37673, Korea

The advent of three-dimensional printing (3DP) technology has enabled the creation of a tangible and complex 3D object that goes beyond a simple 3D-shaded visualization on a flat monitor. Since the early 2000s, 3DP machines have been used only in hard tissue applications. Recently developed multi-materials for 3DP have been used extensively for a variety of medical applications, such as personalized surgical planning and guidance, customized implants, biomedical research, and preclinical education. In this review article, we discuss the 3D reconstruction process, touching on medical imaging, and various 3DP systems applicable to medicine. In addition, the 3DP medical applications using multi-materials are introduced, as well as our recent results.

Index terms: 3D printing; Multi-materials; Personalized treatments; Customized implant; Biomedical research; Preclinical education

INTRODUCTION

The rapid development of medical imaging modalities

such as computed tomography (CT), magnetic resonance imaging (MRI), and various ultrasonic apparatuses has provided improved patient-specific anatomy information while reducing diagnostic invasiveness (1, 2). With the help of advanced image post-processing technologies (3, 4), radiological techniques can be combined with a variety of tools, such as multiplanar reformation, three-dimensional (3D) visualization, and image navigation, which is pivotal in both diagnosis and treatment (4). The advent of 3D printing (3DP) technology, sometimes called rapid prototyping (RP), has provided a more advanced tool with an intuitive and tangible 3D fabricated model that goes beyond a simple 3D-shaded visualization on a flat screen (5).

For its use in medical fields, the most important of the many advantages of 3DP technology is the "zero lead time" between design and final production. Furthermore, compared with industrial approaches, 3D model design for 3DP medical applications is easier, because most can be acquired using 3D surface reconstruction of medical images with

the help of image post-processing. In the clinical setting, the possibility of one-stop manufacturing from medical imaging to 3DP has accelerated the recent medical trend towards "personalized" or "patient-specific" treatment. Secondly, 3DP, as an additive manufacturing technology (6), exhibits the characteristics of "zero constraint and zero skill" for 3D fabrication, which are perfect for medical applications, because the shape of 3D models derived from patient-specific medical images is usually too complex to be manufactured by conventional fabrication methods. Hence, 3DP machines have since the early 2000s been used in a variety of medical applications. The technique has been used mainly for hard tissue applications due to the hardness of most 3D printable materials (7).

The cost of 3DP systems has decreased recently because several 3DP mechanisms have become off-patent. Moreover, as 3D printable multi-materials with transparent, full-colored, and flexible characteristics are now commercially available, 3DP technologies have been applied to various fields of medicine, including personalized treatment, medical research, and premedical education, for both soft and hard tissues (7-10). The present article discusses the generation of 3D reconstructed models, covering medical imaging, the post-processing of 3D models, and the recent developed 3DP systems, and reviews various related medical applications, especially those that use the recently commercialized 3DP technologies and multi-materials.

3D Modeling from Medical Images and Computer-Aided Design

For medical use, after patient scanning by CT and/or MRI, the DICOM data can be exported and processed into stereolithography data files such as stereolithography or other 3D file formats by using segmentation, surface extraction, and 3D model post-processing. Less than a 1-mm CT slice thickness and voxel with isocubic spacing are recommended. The time required depends mainly on the clinical application. In particular, segmentation is a vital procedure for improving the overall accuracy and requires considerable time. No satisfactory fully automated medical image segmentation algorithms have been developed. Therefore, manual or semi-automated segmentation algorithms have generally been used, which have increased the importance of operator experience. After segmentation, a surface model should be generated by a marching cube (11, 12) or other 3D contour extraction algorithm (13). For

medical visualization, these types of shaded surface display techniques are well developed. However, this 3D model itself is not good enough for 3DP, due to, for example, too many mesh units and incomplete topological soundness. Therefore, topological correction (14), decimation (15), Laplacian smoothing (16), and local smoothing (17) are needed to create a 3D model for 3DP. In addition, virtual simulation, including determination of the entry point and direction of the screw and surgical line, is performed for patient-specific surgical planning. Based on such planning, surgical guides are designed using computer-aided design (CAD) software. After generation of a 3D model, the most suitable 3D printer for the application should be selected. The 3D model file is uploaded into the 3D printer. The 3D printer uses layer-by-layer stereolithographic accumulation to fabricate the 3D physical model. The overall procedure is presented in Figure 1. In general, the accuracy of the 3DP object depends on the combination of the accuracy of the medical image, which should be as thin as possible, the appropriate imaging process for 3D modeling, and the 3DP accuracy of the system.

3DP Systems for Medicine

The 3DP technology used in medicine (18) can be classified by the technique, the material, or the aimed deposition process used. The technical type classification includes stereolithography apparatus (SLA), multi-jet printing (MJP), PolyJet printing, digital light processing (DLP), selective laser sintering (SLS), direct metal laser sintering (DMLS), color-jet printing (CJP or binder-jet), fused deposition modeling (FDM), laminated object manufacturing, and electron beam melting. The material classification includes thermoplastic, metal powder, ceramic powder, eutectic metals, alloy metal, photopolymer, paper, foil, plastic film, and titanium alloys. The aimed deposition process classification includes PolyJet printing based on drop-on-drop deposition and FDM based on continuous deposition. We briefly summarize the 3D printers applicable to the medical field in Table 1.

The liquid-based 3DP technology of SLA is the most widely used 3D technique for surgery and was first applied to grafting of a skull defect in 1994 (19). The SLA system consists of a bath of photosensitive resin, a model-building platform, and an ultraviolet (UV) laser for curing the resin (Fig. 2). A computer-controlled mirror is used to focus the UV laser onto the surface of the resin and cure the resin

on a slice-by slice basis. These slice data are fed into the RP machine, which directs the exposure path of the UV laser onto the surface of the resin. The layers are cured sequentially and bind together to form a solid object, beginning from the bottom of the model and building upward. Each new layer of resin is wiped across the surface of the previous layer using a wiper blade before being exposed and cured. The model is then removed from the bath and cured for a further period in a UV cabinet (18). Generally, SL is considered to provide the greatest accuracy and best surface finish of any RP technology. The model material is robust, slightly brittle, and relatively light (20, 21). Choi et al. (20) found that the absolute mean deviation between an original dry skull and an SLA model over 16 linear measurements was 0.62 ± 0.5 mm (0.56 ± 0.39%)

(22). Schicho et al. (22) compared the accuracy of CT and SL models. The accuracy for SL models expressed as the arithmetic mean of the relative deviations ranged from 0.8% to 5.4%, with an overall mean deviation of 2.2%. The mean deviations of the investigated anatomical structures ranged from 0.8 mm to 3.2 mm. An overall mean of deviations (comprising all structures) of 2.5 mm was found.

The liquid-based 3DP technology of MJP uses a print head to disperse an acrylic photopolymer (part) and wax (support) simultaneously. The injected materials are cured by UV light (Fig. 3). In the front view of the equipment, material is injected to the assigned location while the tray moves backward and forward, and they are stacked layer-by-layer in the z-axis. MJP is the highest-precision 3DP technique. The transparency of the main material of the acrylic
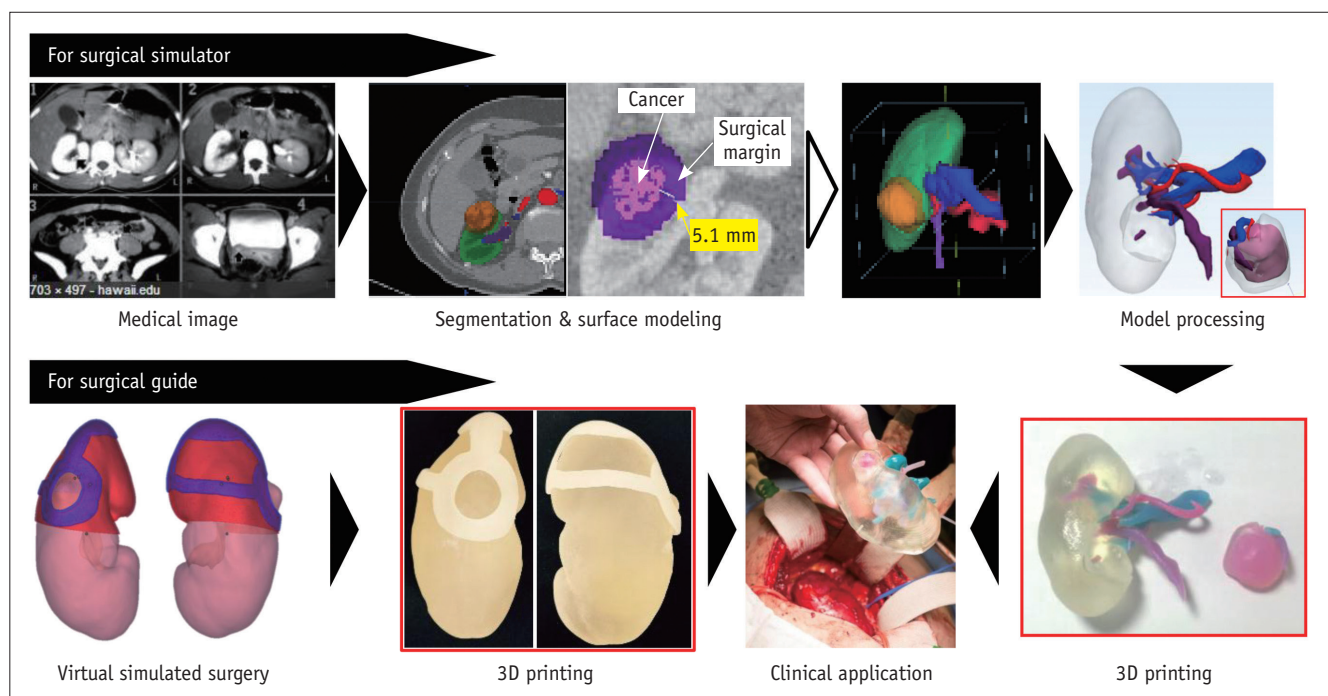

Fig. 1. Overall procedure for 3D printing from medical images. 3D = three-dimensional

Table 1. Summary of 3D Printers with Medical Applications

	FDM	MJP	PolyJet	SLA	CJP	SLS	DMLS
Accuracy	●◐	●●◐	●●◐	●●●	●●	●◐	●◐
Material	Thermoplastic plastics	Photopolymers			Plasters	Thermoplastic plastics, metals, ceramics	Metals
Main application	Phantom	Surgical tool	Phantom	Surgical tool	Phantom	Medical implant	
Cost	$	$$	$$$	$$$	$$	$/$$$	$$$$
Layer thicknesses (mm) (equipment)	0.127–0.330 (Fortus 450 mc)	0.016 (ProJet 3510)	0.016 (Connex series)	0.025–0.050 (ProJet 6000)	0.1 (ProJet 460)	0.08–0.15 (ProX 500), 0.09 (EOS M 400)	0.02 (ProX 300)

CJP = color-jet printing, DMLS = direct metal laser sintering, FDM = fused deposition modeling, MJP = multi-jet printing, SLA = stereolithography apparatus, SLS = selective laser sintering, 3D = three-dimensional

photopolymer resins can be controllable but its strength is relatively weak. In addition, shape deformation occurs at 65 degrees or more.

PolyJet printing is performed by jetting state-of-the-art photopolymer materials in ultra-thin layers of 16 µm onto a build tray layer-by-layer until the model is completed. Each photopolymer layer is cured by UV light immediately after it is jetted, producing fully cured models that can be handled and used immediately without post-curing (Fig. 4). A gel-like support material that is specially designed to maintain complicated geometries and is easily removed by hand and water jetting is used (18). In fact, there is little difference between the MJP and PolyJet methods. PolyJet printing can avail of a variety of materials, including a rubber-

like material, and its post-processing stage is shorter and simpler. At present, this technique is overly time consuming and, therefore, too expensive to be used in surgical applications. Ibrahim et al. (23) reported a dimensional error of 2.14% when reproducing a dry mandible using this technique (23).

The liquid-based 3DP method of DLP uses a conventional DLP projector as a light source. In the first step, it projects a two-dimensional (2D) image into a light-curable resin in a vat (Fig. 5). This method shows excellent surface finish and the fastest printing. The mechanical properties of the used material are good but the type of material and its color are limited. Moreover, the material and printing system are expensive.

The powder-based 3DP technology of SLS uses a CO_2 laser beam to selectively fabricate models in the following way. First, the 2D slice data are fed into the SLS machine, which directs the exposure path of the laser over a thin
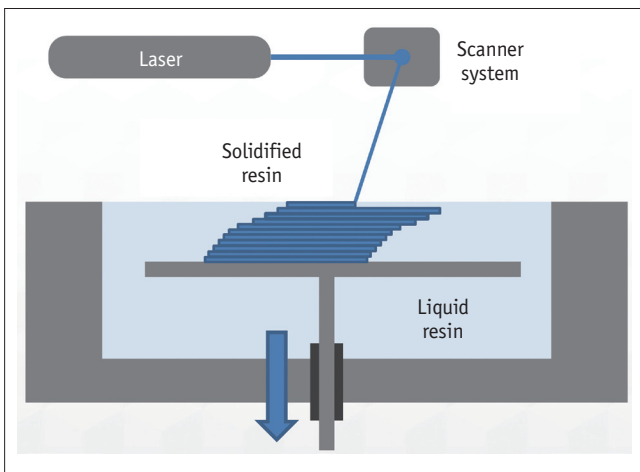
Fig. 2. Basic principle of stereolithography apparatus method.
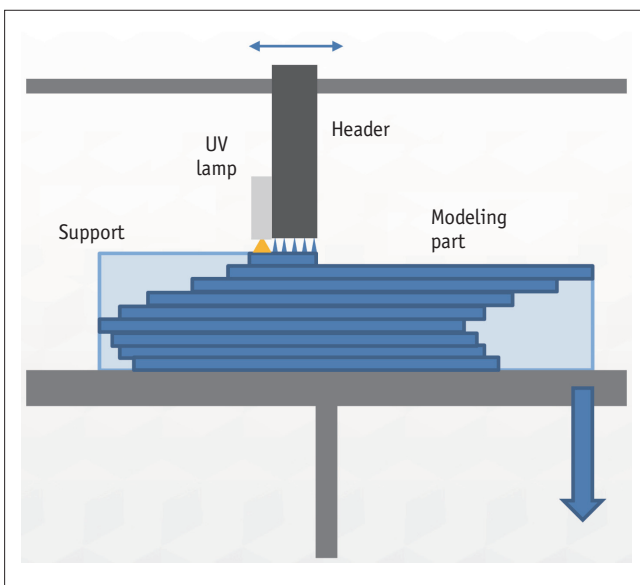
Fig. 3. Basic principle of multi-jet printing method. UV = ultraviolet
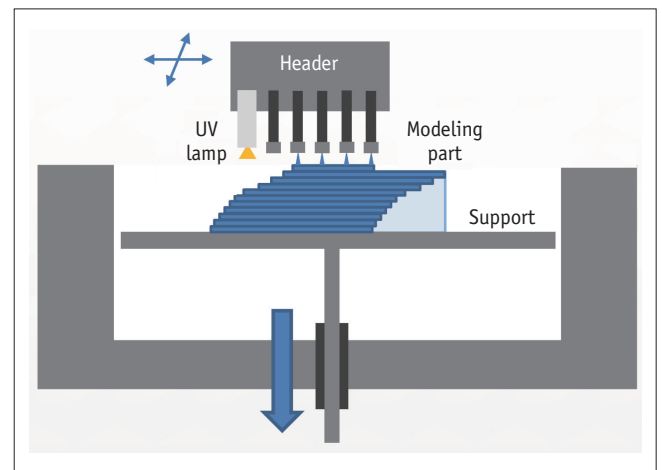
**Fig. 4. Basic principle of PolyJet method.** UV = ultraviolet
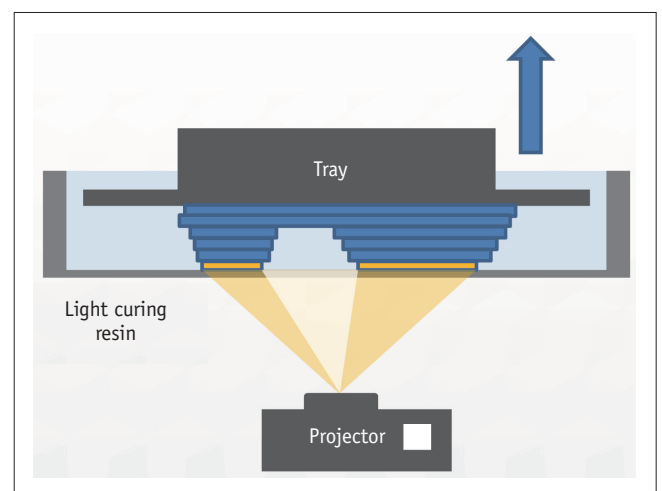
Fig. 5. Basic principle of digital light processing method.

layer of powder previously deposited on the build tray and leveled with a roller (Fig. 6). The laser heats the powder particles, fusing them to form a solid layer, and then moves along the X and Y axes to design the structures according to the CAD data. After the first layer fuses, the build tray moves downward, and a new layer of powder is deposited and sintered. The process is repeated until the object is completed. The prototype surface is finished by sandblasting (18). The SLS prototype is opaque, and its surface is abrasive and porous. The prototype fabrication time is 15 hours. The accuracy of the SLS model is relatively high, with maximum standard errors of 0.1 to 0.6 mm. Because of the high cost of the materials, several parts are fabricated simultaneously. The long fabrication time for the SLS technique (16 hours) is similar to that required for fabrication with the SL system (24). The equipment is expensive, but a low-cost SLS system (Norge Company, Seynod, France) was recently developed due to patent expiration.

The powder-based 3DP method of the DMLS technique uses a solid-state Yb fiber laser beam to selectively fabricate models in the following way (25). DMLS was first developed by the EOS Company. The method is similar to that of SLS (26) and selective laser melting, with the exception of the melting degree of the material; small variations result in marked alteration of the characteristics of the material. A variety of materials–such as aluminum, cobalt, steel, nickel alloy, stainless steel, and titanium–can be used in DMLS. Because the powder used plays a role in supporting the model, post-processing, including supporter removal, is not needed. In addition, its printing quality is generally excellent.
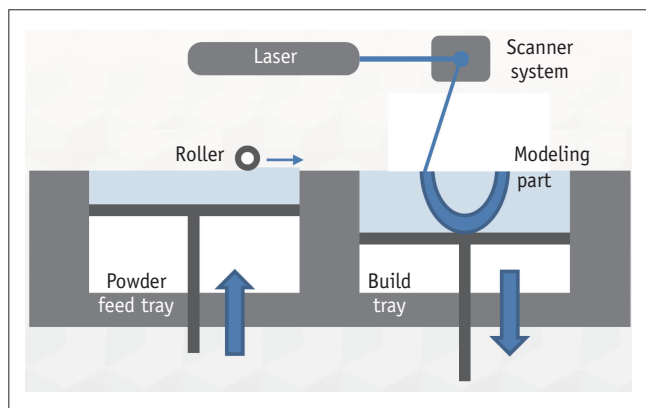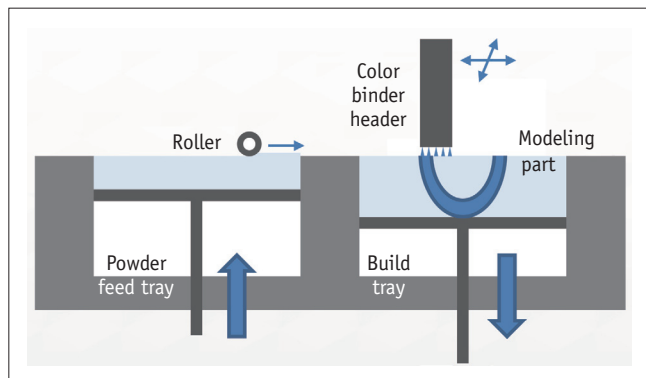
The CJP method uses a print head to selectively disperse a binder onto powder layers. This technology has a lower cost than similar techniques. First, a thin layer of powder is spread over a tray using a roller, similar to that used in the SLS system (Fig. 7). The print head scans the powder tray and delivers a continuous jet of a solution that binds the powder particles as it touches them. No support structures are required while the prototype is being fabricated, because the surrounding powder supports the unconnected parts. When the process is complete, the remaining surrounding powder is aspirated. In the finishing process, the prototype surfaces are infiltrated with a cyanoacrylate-based material to harden the structure (24). The printing technique enables the formation of complex geometrical structures, such as hanging partitions inside cavities, without artificial support structures (18). Because it uses a CMYK color ink cartridge, as used in conventional 2D printers, the 3D fabricated object can be printed with an almost identical range of color. The printing and infiltration processes require ~4–6 hours. The 3D printers used in this process are relatively inexpensive (25000 British pound [GBP]), have fast build times (4 hours for a full skull), and are easy to maintain. Additionally, these 3D printers are cost effective (1 GBP/cm^3), associated with low waste, accurate (± 0.1 mm in the Z plane, ± 0.2 mm in the X and Y planes), have small dimensions, and can produce hard, soft, and flexible models. These printers can also be used to identify different types of body tissue depending on the predefined threshold setting selected. Silva et al. (24) reported a mean dimensional error of 2.67% in prototypes produced using 3DP technologies compared with a dry human skull (24).

The solid-based 3DP technology of FDM uses a similar principle to SL in that it builds models on a layer-by-layer basis. The main difference is that the layers are deposited as a thermoplastic that is extruded from a fine nozzle. A commonly used material for this procedure is acrylonitrile butadiene styrene (ABS). The 3D model is constructed by

Fig. 6. Basic principle of selective laser sintering method.

Fig. 7. Basic principle of color-jet printing method.

extruding the heated thermoplastic material onto a foam surface along a path indicated by the model data (Fig. 8). Once a layer has been deposited, the nozzle is raised by between 0.278 to 0.356 mm and the next layer is deposited on top of the previous layer. This process is repeated until the model is completed (18). As with SL, support structures are required for FDM models because time is needed for the thermoplastic to harden and the layers to bond together (27). The supports can be removed by a simple tool or can be dissolved using a special acidic solution. Although it is the most popular 3D printer technology, the surface finish is relatively poor. Hence, several post-processing options, including acetone fumigation, can be used.

Medical Applications

Since the early 2000s, 3DP technologies have been used in a variety of medical fields, from 3D phantoms for simulation to bioprinting of organs. The former can be used in personalized treatments that take into account patient-specific anatomical variations. Personalized treatment makes use of 3DP in surgical planning and simulation, surgical guidance, and implantable device creation. 3DP has also been used in various scientific studies in the biomedical field. Personalized or disease-specific 3DP phantoms can be used to better understand physiological problems. Finally, 3DP has been used for educational and training purposes.

Applications for Personalized Treatment

Surgical Planning and Guidance Tools
In surgical planning and operating processes for personalized treatment, 3D-printed patient-specific phantoms and surgical guides have recently been used
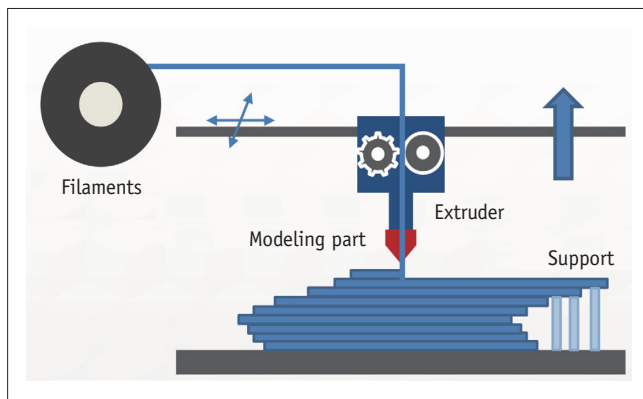

Fig. 8. Basic principle of fused deposition modeling method.

increasingly frequently to enhance understanding complex procedures and to simplify the operating procedure. These phantoms assist diagnosis and pre-surgical planning. In addition, 3DP surgical guides made of temporary biocompatible materials can be attached to the surface of the hard or soft organ by 3D modeling of the surgical interface through the pre-surgical planning. To date, the benefit of 3DP for surgical planning and as a guidance tool has been demonstrated in various hard tissue surgical applications, such as craniofacial and maxillofacial surgery (28-33), spine surgery (34), cardiovascular surgery (35, 36), neurosurgery (37, 38), pelvic surgery (39, 40), and visceral surgery (41).

Recently, as transparent, full-color, and flexible 3D printable materials have become available, the level of realism of the 3D phantoms for surgical planning and treatment of soft organs has improved significantly. Increased diversity due to improved transparency, color, and softness facilitates improved comprehension of complex 3D anatomical structures and guidance functions for soft tissues (42). Yang et al. (43) used a full-colored and flexible 3DP phantom as a pre-planning simulator for extended septal myectomy. From the cardiac CT data, a myocardial 3D model was generated using in-house software (A-view Cardiac; Asan Medical Center, Seoul, Korea). Using a 3D printer (Connex3 Objet500; Stratasys Corporation, Rehovot, Israel), the left ventricular (LV) myocardium, papillary muscle, and intraventricular muscle band (including accessory papillary muscle) were manufactured using differently colored materials, whose flexibility could be controlled by adding a rubber-like and transparent material (Fig. 9). The authors stated that the 3DP phantom provided intuitive information on the LV geometry, including the extent of the hypertrophied septum, and the location and length of the papillary muscle and intraventricular muscle band, which enabled preoperative simulation of the surgical myectomy.

Transparent 3D printed kidney phantoms have been used to enhance preoperative planning and intraoperative orientation of risk structure and target tissue in partial nephrectomy. All renal units with renal mass were modeled using in-house software (A-view; Asan Medical Center, Seoul, Korea), which also provides information on the renal anatomy, mass, and volume (Fig. 10). The virtual resection simulation followed an adequate safety margin with −5 mm distance from the renal mass. 3D-printed kidney phantoms were fabricated using a 3D printer (Connex3 Objet500;
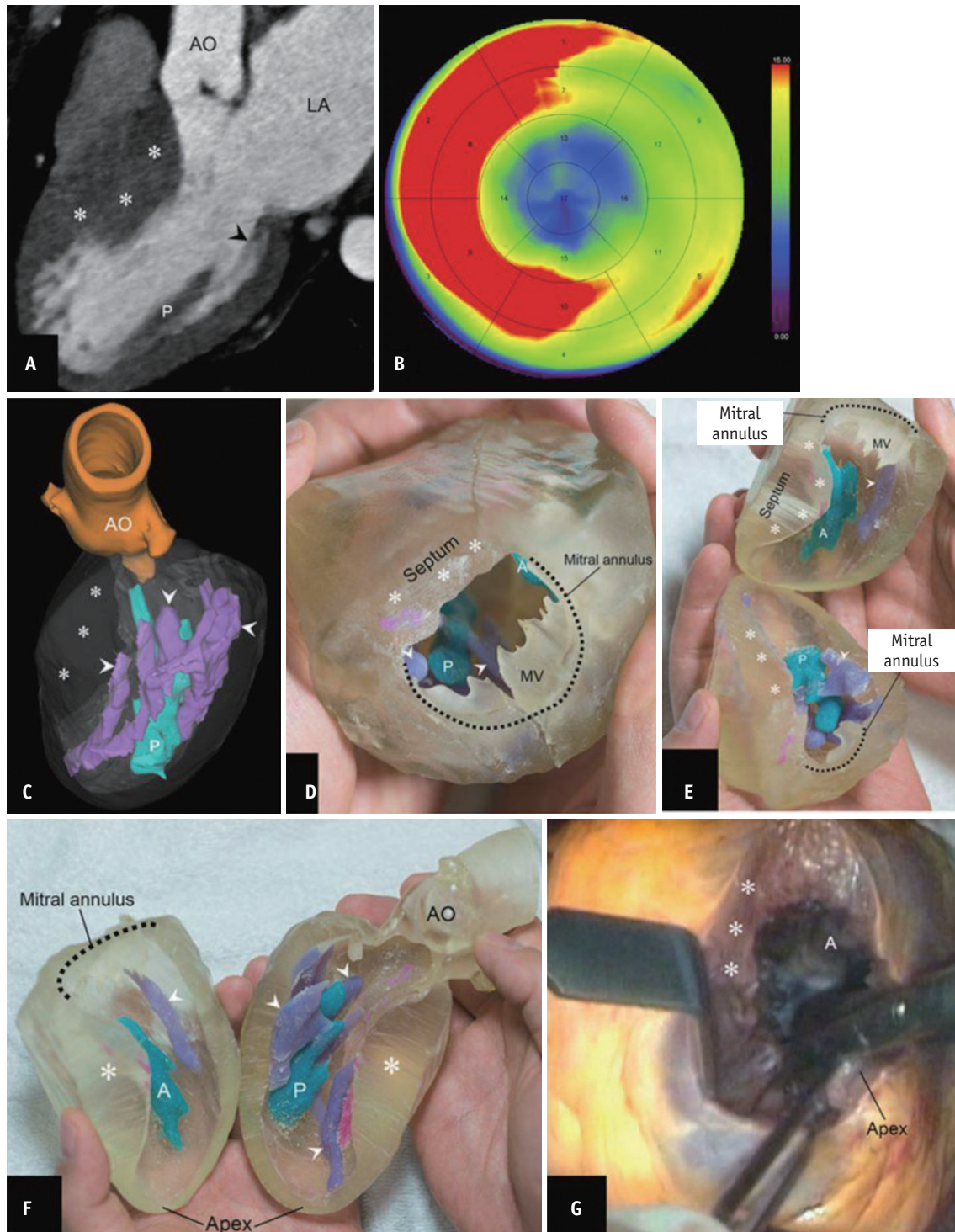
Fig. 9. 3D-printed simulator for extended septal myectomy.
A. Cardiac three-chamber CT image showing hypertrophied interventricular septum (asterisks), posterior papillary muscle (P), and intraventricular muscle band or accessory papillary muscles (arrowhead). **B.** Bull's-eye map generated using end-diastolic phase of CT imaging shows extent of hypertrophied myocardium (red area, > 15 mm in thickness). **C.** 3D reconstructed model. **D-F.** 3D-printed phantom of myocardium showing geometric relationships among hypertrophied septum (asterisks), papillary muscle (A = anterior, P = posterior), and intraventricular muscle band (asterisks). **G.** Intraoperative photography via apical approach shows limited visual field of LV cavity. Base of anterior papillary muscle is exposed after excision of muscle band (not shown) near anterior papillary muscle. Adapted from Yang DH et al. *Circulation* 2015;132:300-301, with permission of Wolters Kluwer Health, Inc. (43). AO = aorta, LA = left atrium, LV = left ventricle, MV = mitral valve, 3D = three-dimensional
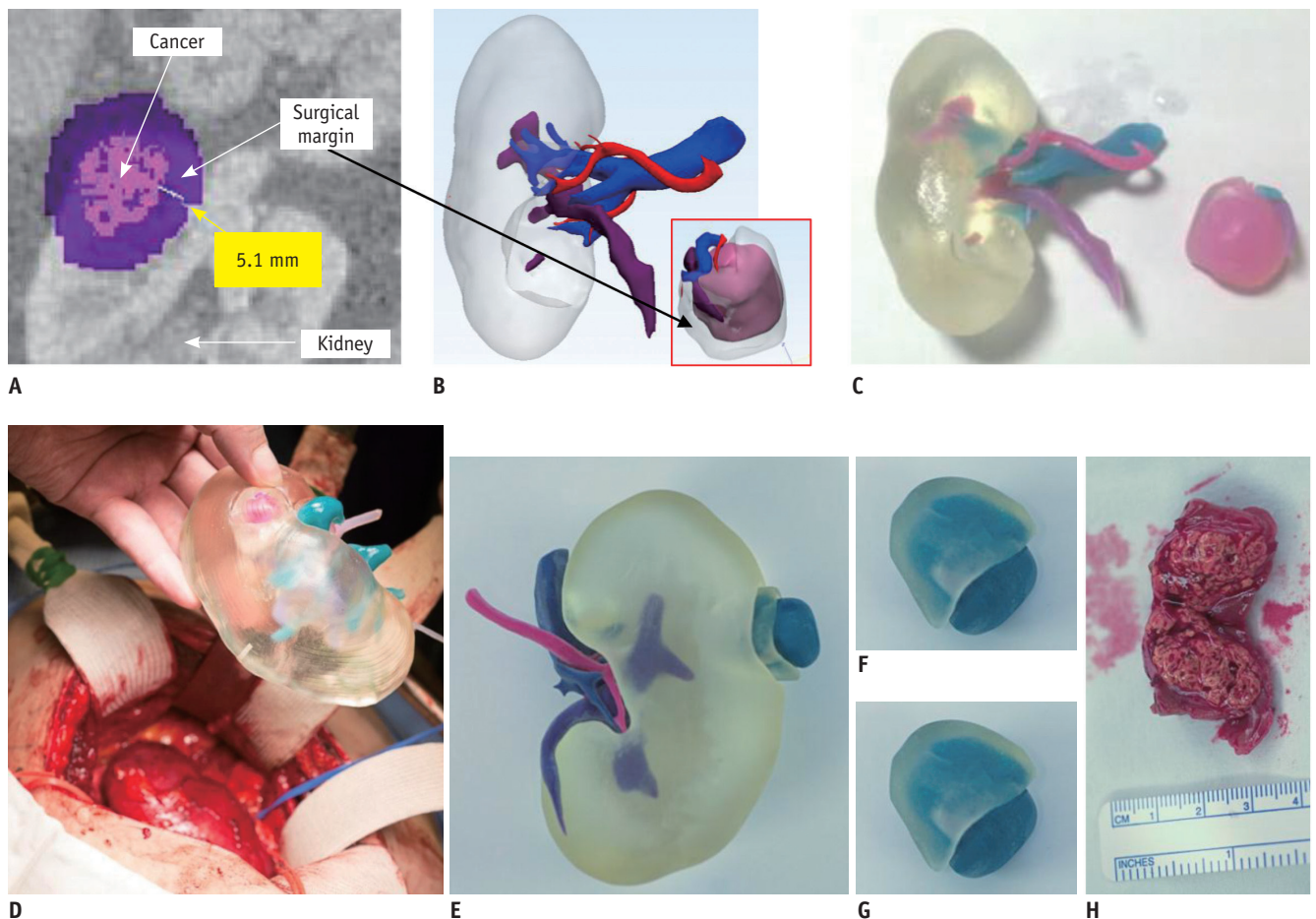
Fig. 10. 3DP application in partial nephrectomy.
A. CT-image-based modeling of renal cell carcinoma and safety margin for carcinoma surgery. **B.** 3D-reconstructed model of all renal units with renal mass, which includes safety margin. **C.** 3D-printed phantom. Part of carcinoma including safety margin can be separated. **D.** Photograph of 3DP phantom in operating room. **E-H.** Another case of 3DP phantom used in surgery. 3DP phantom and real renal mass were compared after partial nephrectomy. 3DP = three-dimensional printing

Stratasys Corporation, Rehovot, Israel). The 3DP phantoms were used to improve surgical outcome and may also improve the patient's understanding of their disease and improve satisfaction.

Even the softest 3D printable materials cannot be directly used as surgical simulators because they are too hard for scalpel incision and suturing. Therefore, additional post-processing using gelatin or silicon molding techniques or a novel 3DP system that can directly jet a variety of silicon materials needs to be developed.

Implantable Devices

Three-dimensional printing techniques are also used in implant design to create patient-specific prostheses, which open new treatment opportunities for patients outside the standard range of ready-made commercial implants. In addition, this approach has improved surgical

performance by enabling the creation of patient-specific anatomy-based implants (7). For hard tissue structures, metal implants have, in particular, been successfully used for various applications (44, 45), most of which were Food and Drug Administration approved, such as mandible (33) and dental (46) restoration and hip (47), femoral (48), and hemi-knee joint reconstruction (44, 45). In addition, the biocompatible ceramic hydroxyapatite (49) and the biodegradable polymer polycaprolactone (50) have been used in 3DP-based applications to replace hard tissues with customized implants.

Beyond hard tissue applications, customized implants created using 3DP have recently been used in the interventional field. Amerini et al. (51) demonstrated the feasibility of a personalized interventional treatment for tricuspid regurgitation using a braided stent in an animal study. Using cardiac CT data, a 3D reconstructed model
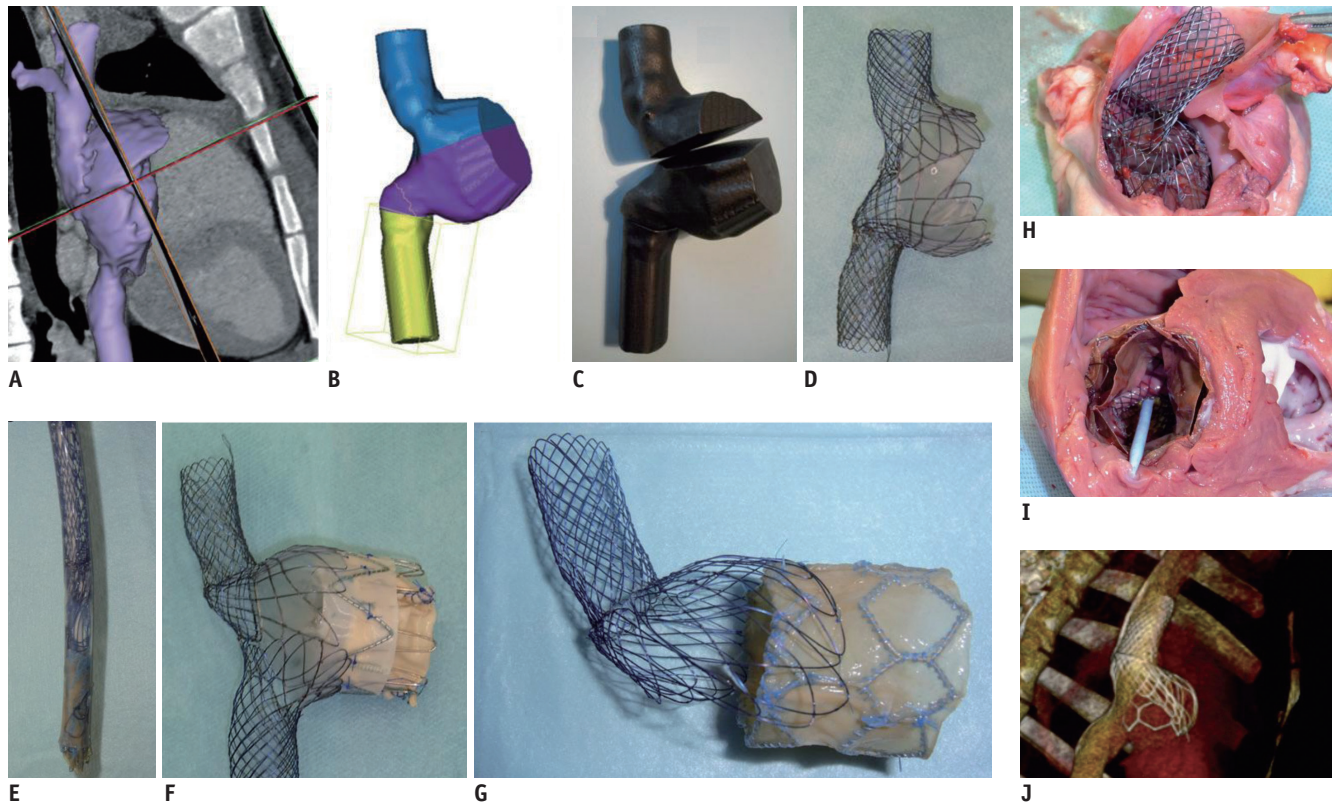
Fig. 11. 3D printing-mold-based personalized stent.
A. CT-based primary three-dimensional (3D) reconstruction. B. 3D-reconstructed model of main structural parts. C. 3D-printed phantom mold of main structural parts with Alumide material. D. Personalized stent with nitinol material. E. Equipped state of developed stent in introducer. F, G. Two different prototypes equipped with self-expanding bio-prosthetic valve. H-J. Results of animal study that involved implantation of developed stent. Post-mortem autopsy (H, I) and CT fluoroscopy (J) revealed accurate positioning of valve prostheses. Adapted from Amerini et al. *Interact Cardiovasc Thorac Surg* 2014;19:414-418, with permission of Oxford University Press (51).

of the right-sided cardiac cavities of a pig was obtained (OsiriX® Imaging Software; Pixmeo, Switzerland). A solid Alumide® mold was manufactured using a 3DP system and a personalized compressible nitinol stent was then subsequently produced and fitted onto the 3DP mold (Fig. 11). This customized stent was almost completely fitted onto the right atrium and an additional tubular stent component containing a tissue valve prosthesis was developed. From the feasibility study conducted in animals, they found that the 3DP-based stent could stabilize the biological valve prostheses by force transmission from the annulus to the atrial wall and the adjacent vena cava.

Another example of a 3DP-based medical implantable application is the use of medical-grade silicon material for soft tissue. Figure 12 shows a pilot study to develop a patient-specific soft implant for filling a dead zone of lung after pneumonectomy. From the CT data, the volume of the dead zone was three-dimensionally reconstructed (A-view, Asan Medical Center). In this pilot study, a 3D printer system (Fortus 250 mc, Stratasys Corporation, Eden Prairie, MN, USA) was used to manufacture the patient-specific phantom of the dead zone, which was used as a mold to produce a negative mold with silicon material. The final dead zone phantom with silicon material was cast by using the negative mold and the softness of the 3D-printed material was evaluated by clinicians. In the near future, the final implantable device could be manufactured using a medical-grade silicon material through an additional molding process and evaluated in a prospective clinical trial.

In this article, only clinical applications that can be realized by the already developed 3DP technologies are discussed, but there are other approaches for personalized implants, including bio-printing of tissues and organs (10, 52, 53) and organ-on-a-chip (54, 55).

Phantom Fabrications for Medical Research

For better understanding of complex pathologies, a variety of *in vitro* and *ex vivo* studies have investigated phantoms fabricated by 3DP (56-59). These tangible 3DP
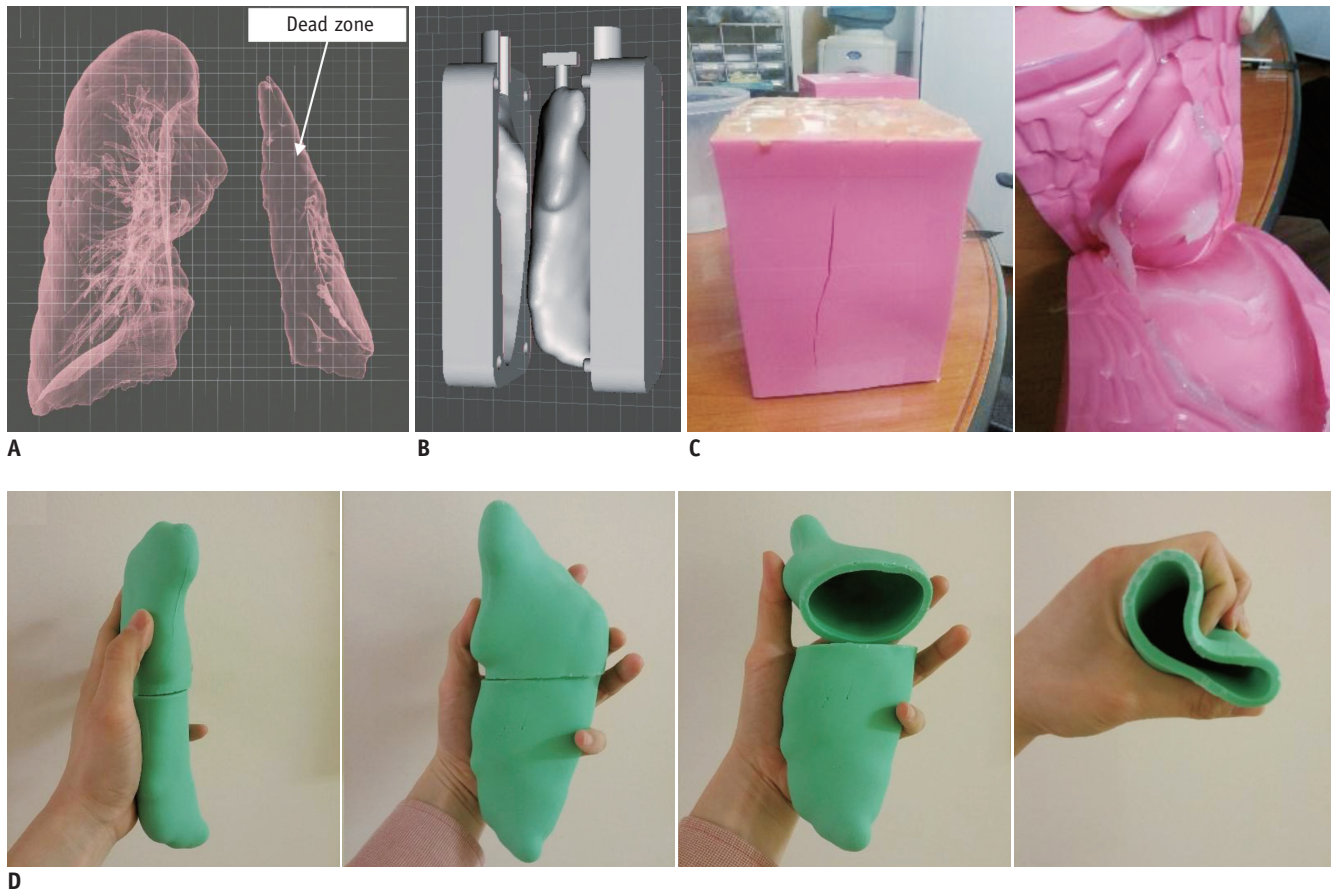
Fig. 12. Pilot study of patient-specific implant device with flexible material.
A. CT-based three-dimensional (3D) reconstruction of patient-specific dead zone after pneumonectomy. **B.** 3D-modeled dead zone and frame for molding. **C.** Fabricated negative mold with silicon material. **D.** Final product of spacer for dead zone with silicon material using molding technique.
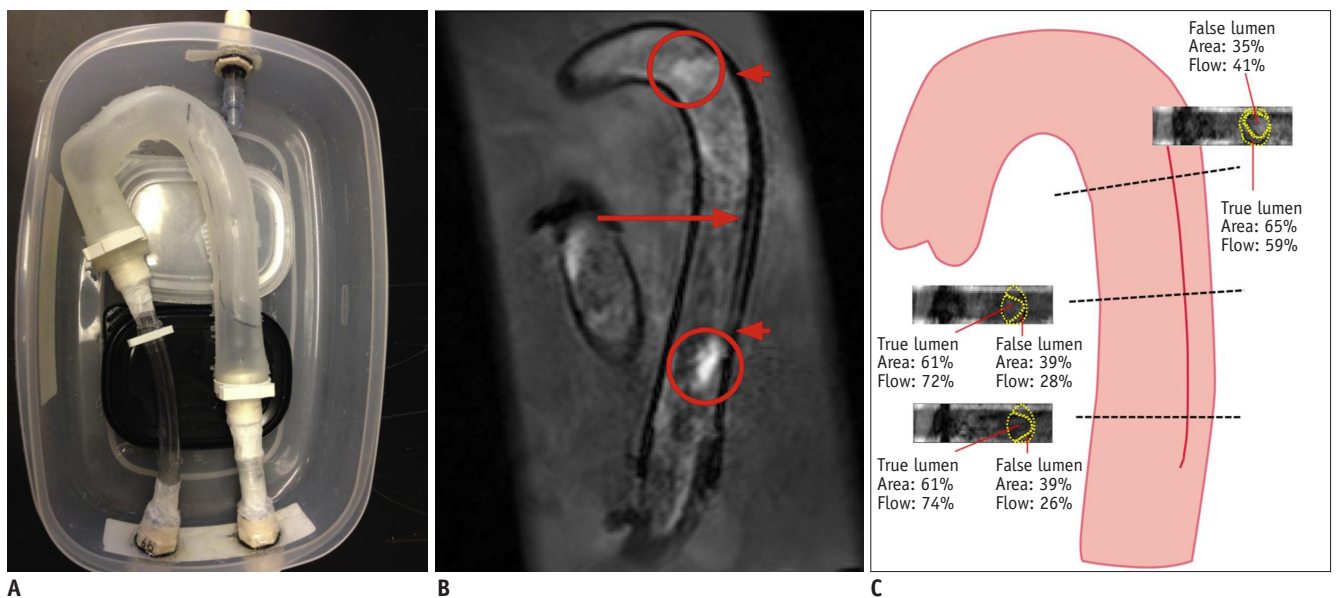
Fig. 13. 3DP-mold-based phantom for aortic dissection.
A. 3DP-based silicone phantom of aortic dissection. Adapted from Veeraswamy RK et al. *J Vasc Surg* 2015;61:128S-129S, with permission of Elsevier (64). **B.** Four-dimensional flow MRI image showing intimo-medial flap (arrow and arrowheads); flow is directed horizontally into true lumen at both entry and exit tears during diastole. Adapted from Birjiniuk J et al. *J Surg Res* 2015;198:502-507, with permission of Elsevier (63). **C.** Cross-sectional velocity fields at true and false lumina in representative axial plan. 3DP = three-dimensional printing

phantoms themselves provide more intuitive information than mere 3D visualizations. Furthermore, various *in vitro* studies have been more beneficial, such as for assessing the hemodynamics or aerodynamics of cardiovascular or airway diseases (60, 61), because abnormal interactions between fluids and organs in a disease model can be delicately investigated through patient-specific fluid phantom studies. The detailed fluid dynamic information, including that of disease models, provided by these experimental studies may also facilitate postoperative simulation for clinicians.

A 3D compliant model mimicking the elastic properties of vessels has also been manufactured using silicon or polyurethane material (35, 62). Recently, a descending aortic dissection phantom fabricated by 3DP used a two-mold process to mimic the intimal flapping motion of aortic dissection (63, 64). From the CT data, a 3D reconstructed model of descending aortic dissection was generated and modified to manufacture a 3DP mold for silicon casting (Fig. 13). A 0.5 mm layer was first cast on the true lumen mold, and the second casting was then performed over the initial

cast to produce the false lumen. Four-dimensional flow MRI was used to quantitatively measure the local velocity profiles of both lumens.

In addition, a fluid dynamic study of paramedian pontine infarction caused by atheroma obliteration of the perforators of the basilar artery (BA) was performed. Using the MRI data, a stenotic BA model was generated using dedicated software (A-view; Asan Medical Center) and was then 3D printed with ABS thermoplastic material by a 3DP system (Fortus 400 mc; Stratasys Corporation) (Fig. 14). The 3DP BA phantom was cast with a polydimethylsiloxane (PDMS) silicone compound, and then the ABS material was dissolved out from the PDMS in acetone. The fabricated PDMS phantom with a hollow BA artery morphology was applied to a fluid dynamic experiment using particle image velocimetry, which is a quantitative velocity field measurement technique that uses optical scanning. This experimental study verified the hypothesis (65) that perforator infarction can be caused by a hemodynamic mechanism that is triggered by stenosis-induced
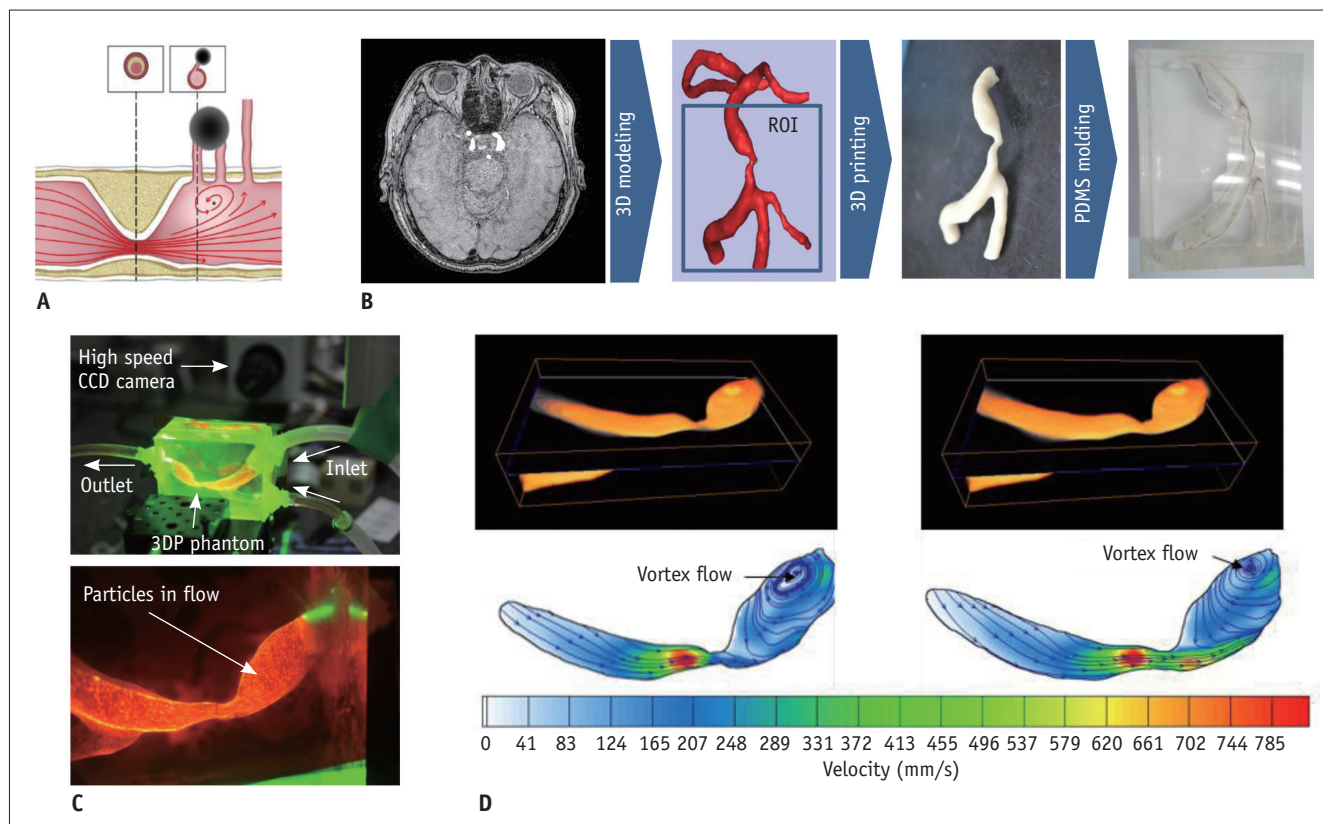
Fig. 14. Fluid dynamic study of paramedian pontine infarction.
A. Schematic of mechanism for generating PPI. Adapted from Kim BJ et al. *J Stroke Cerebrovasc Dic* 2014;23:1991-1993 (65). **B.** Fabrication of transparent patient-specific BA phantom for optical flow measurement. **C.** Experimental setup of PIV measurement using manufactured BA phantom. **D.** Quantitative hemodynamic information of velocity field and vortex position in poststenotic area of BA. BA = basilar artery, PDMS = polydimethylsiloxane, PIV = particle image velocimetry, PPI = paramedian pontine infarction, 3DP = three-dimensional printing

recirculation flow in the poststenotic area.

Simulation for Medical Education and Training

Traditionally, human cadavers have been used to teach students anatomy and the morphological relationships of various organs in medicine. Using this approach, however, it is difficult to accumulate sufficient experience of surgery for a variety of diseases. Assisting and observing surgical operations gives a trainee indirect experience, but this approach is insufficient to improve operating skills and intuitive understanding of complex pathologic and disease-specific anatomical details, especially in surgeries that use laparoscopy and endoscopy. Hence, many trainees must develop their surgical skills during real surgical procedures. In addition, it is increasingly difficult to dissect human cadavers or observe medical treatment, for such reasons as cultural disapproval of dissection of the human body and enhanced patient rights.

Patient-specific 3D models fabricated by the 3DP system have been used to train young surgeons in surgical procedures, including bone surgery (66), endovascular stent implantation (35, 62, 67, 68), and *ex vivo* biliary drainage surgery (59). The recently developed multi-material 3DP technology provides more realistic phantoms that mimic real hard and soft tissues (69, 70). Waran et al. (69) used multi-material neurosurgical phantoms with a pathological entity with varying consistencies and densities for their trainees (Fig. 15). Based on the CT data, in-house software (Biomodroid; CBMTI, Universiti of Malaya, Malaysia) was used to generate a 3D reconstructed model of the skin, bone, dura, and tumor and manufactured 3DP phantoms using a 3D printer (Objet500; Stratasys Corporation, Rehovot, Israel). They stated that their trainees could practice the basic steps from navigation and planning of skin flaps to the initial steps in a craniotomy and simple tumor excision. Similarly, a 3DP phantom for training in the transcatheter aortic valve implantation (TAVI) procedure was demonstrated (Fig. 16). From the cardiac CT data, LV with a calcified bicuspid aortic value and aorta covering the catheterization root was reconstructed in 3D using dedicated software (A-view Cardiac; Asan Medical Center). Using a 3D printer (Connex3 Objet500; Stratasys Corporation), a 3DP phantom with multi-materials was manufactured in which the soft tissue of the aorta and leaflet was composed of flexible material and the calcification comprised hard material for a more-accurate representation of the *in vivo* situation. Catheterization intervention using a TAVI (SAPIEN; Edwards Lifesciences Corporation, Irvine, CA, USA) was simulated using the fabricated 3DP phantom.

In addition, a 3DP phantom with multi-materials could provide trainees and/or surgeons with various educational and/or rehearsal simulators based on both patient-specific and disease-specific anatomy. By training and/or rehearsing with these simulating phantoms, trainees and/or surgeons may gain confidence before performing real operations.

Discussion and Conclusion

With the development of inexpensive 3D printers, 3D printable multi-materials, and 3D medical imaging modalities, 3DP medical applications have come into the spotlight. Due to the availability of transparent, full-
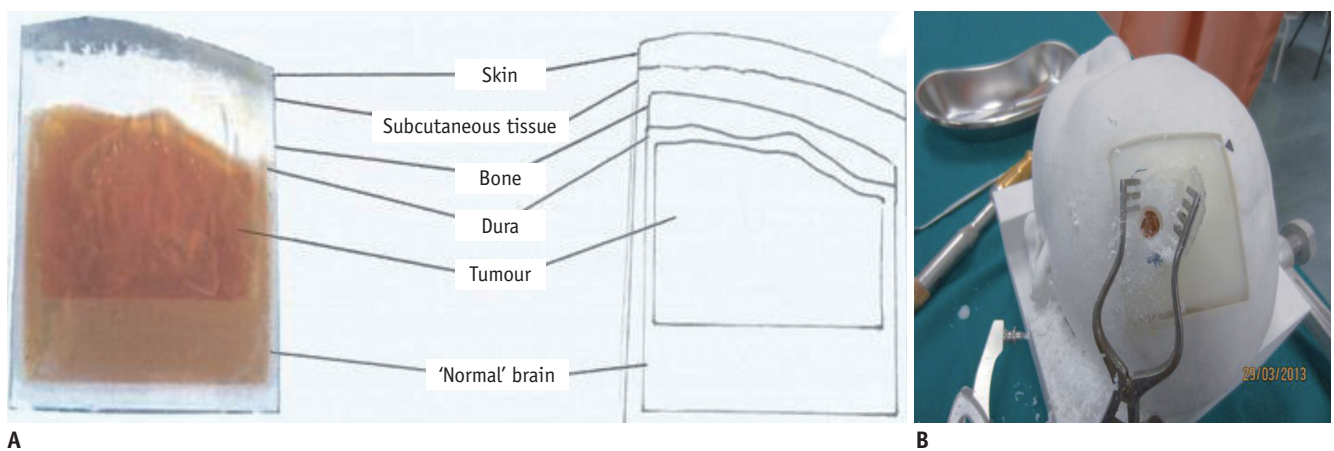

Fig. 15. Neurosurgical phantoms with pathological entity.
A. Cross-sectional view of 3DP phantom and drawing of parts thereof. **B.** Photograph showing burr hole with intact dura in training procedure. Adapted from Waran V et al. *J Neurosurg* 2014;120:489-492, with permission of JNSPG (69). 3DP = three-dimensional printing
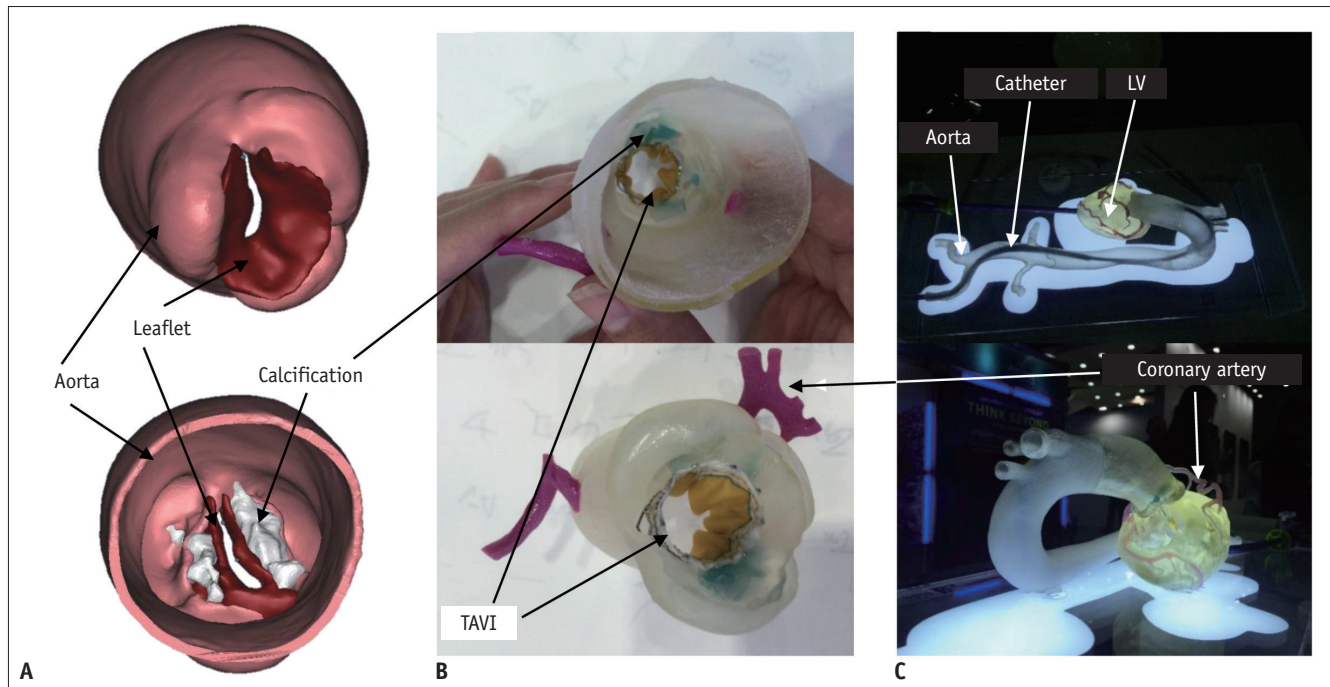
Fig. 16. 3DP phantom for training in transcatheter aortic heart valve implantation.
A. 3D reconstructed model based on real case. **B.** Multi-material 3DP phantom for TAVI. **C.** Simulation of catheterization for TAVI stent showing aortic valve 3DP phantom with TAVI stent inside. LV = left ventricular, TAVI = transcatheter aortic valve implantation, 3DP = three-dimensional printing

colored, and flexible multi-materials, 3DP objects can be more realistic, mimicking the properties of the real body; i.e., not only hard tissue alone but also hard and soft tissue together.

Regarding applications for personalized medical treatments, 3DP multi-materials could provide a flexible LV phantom for pre-planning of extended septal myectomy (43) and kidney phantoms for a partial nephrectomy simulator. Beyond a surgical guide for hard tissue (30), a surgical guide with flexible material could be used in partial carcinectomy of soft organs. Regarding implantable devices, a recent study showed that 3DP-based personalized stents could be used for tricuspid regurgitation (51). In addition, a patient-specific flexible implant for filling a dead zone in the lung after pneumonectomy with a nonmedical-grade silicon material was developed. It is expected that a final implantable device composed of a medical-grade silicon material could be manufactured by means of an additional molding process. Fabrication of a phantom using a variety of 3DP methodologies for various biomedical research applications would also be useful. By applying a two-mold process to a fabricated 3DP phantom, a flow phantom constructed for descending aortic dissection that mimics the intimal flapping motion could be manufactured (63). Through this patient-specific *in vitro* phantom study,

detailed hemodynamic information on the aortic intima layer could be acquired, which would facilitate postoperative simulation for clinicians. 3D-printable multi-materials have been used to manufacture various educational phantoms. A recent neurosurgical phantom was capable of mimicking the skin, bone, dura, cerebral parenchyma, and tumor using a mixture of soft and hard materials of various colors (69). A more-realistic material is needed to mimic a variety of real soft tissues, but this limitation can be resolved by a hybrid of the 3DP and molding techniques and using materials with enhanced properties (elasticity, tensile strength, compression strength, and fatigue failure). For trainees, these 3DP educational phantoms would play an important role in filling the gap between preclinical studies and real surgery.

Despite the substantial increase in the number of 3DP medical applications, several major limitations, such as those associated with the technology and the time and cost of manufacturing 3D phantoms, remain to be overcome. Development and optimization of the entire procedure, from image acquisition to 3DP fabrication, are required for personalized treatment, even in emergency situations. In addition, it is important to select a specific medical situation with a clear clinical implications, so that the additional costs of 3DP are outweighed by the improved rate

of success and shortened operative duration. Furthermore, to produce an effective 3DP object, multidisciplinary knowledge of the entire 3DP process chain is needed; namely, image acquisition using a protocol suitable for 3D modeling, post-processing of the medical images to generate a 3D reconstructed model, 3DP manufacturing with an appropriate 3DP technique, and post-processing of the 3DP object to adapt it for medical use. We did not focus on bio-printing in this review due to a lack of radiologic relevance, but the developing technologies of bio-printing for tissues and organs (10, 52, 53) and organ-on-a-chip (54, 55) should be noted.

In this article, we illustrate the practical medical applications of 3DP based on currently available 3DP technologies. It is hoped that this review article will enhance understanding of the various 3DP medical applications and facilitate their incorporation into clinical practice.

REFERENCES

1. Kido T, Kurata A, Higashino H, Sugawara Y, Okayama H, Higaki J, et al. Cardiac imaging using 256-detector row four-dimensional CT: preliminary clinical report. *Radiat Med* 2007;25:38-44
2. Meaney JF, Goyen M. Recent advances in contrast-enhanced magnetic resonance angiography. *Eur Radiol* 2007;17 Suppl 2:B2-B6
3. Doi K. Diagnostic imaging over the last 50 years: research and development in medical imaging science and technology. *Phys Med Biol* 2006;51:R5-R27
4. Kirchgeorg MA, Prokop M. Increasing spiral CT benefits with postprocessing applications. *Eur J Radiol* 1998;28:39-54
5. McGurk M, Amis AA, Potamianos P, Goodger NM. Rapid prototyping techniques for anatomical modelling in medicine. *Ann R Coll Surg Engl* 1997;79:169-174
6. Wong KV, Hernandez A. A review of additive manufacturing. *ISRN Mechanical Engineering* 2012 Jun 17 [Epub]. http://dx.doi.org/10.5402/2012/208760
7. Rengier F, Mehndiratta A, von Tengg-Kobligk H, Zechmann CM, Unterhinninghofen R, Kauczor HU, et al. 3D printing based on imaging data: review of medical applications. *Int J Comput Assist Radiol Surg* 2010;5:335-341
8. Gross BC, Erkal JL, Lockwood SY, Chen C, Spence DM. Evaluation of 3D printing and its potential impact on biotechnology and the chemical sciences. *Anal Chem* 2014;86:3240-3253
9. Michalski MH, Ross JS. The shape of things to come: 3D printing in medicine. *JAMA* 2014;312:2213-2214
10. Murphy SV, Atala A. 3D bioprinting of tissues and organs. *Nat Biotechnol* 2014;32:773-785
11. Lorensen WE, Cline HE. Marching cubes: a high resolution 3D surface construction algorithm. *SIGGRAPH Comput Graphics* 1987;21:163-169
12. Tiede U, Höehne KH, Bomans M, Pommert A, Riemer M, Wiebecke G. Investigation of medical 3D-rendering algorithms. *Comput Graphics Appl* 1990;10:41-53
13. Yushkevich PA, Piven J, Hazlett HC, Smith RG, Ho S, Gee JC, et al. User-guided 3D active contour segmentation of anatomical structures: significantly improved efficiency and reliability. *Neuroimage* 2006;31:1116-1128
14. Shattuck DW, Leahy RM. BrainSuite: an automated cortical surface identification tool. *Med Image Anal* 2002;6:129-142
15. Schroeder WJ, Zarge JA, Lorensen WE. Decimation of triangle meshes. *SIGGRAPH Comput Graphics* 1992;26:65-70
16. Field DA. Laplacian smoothing and Delaunay triangulations. *Commun Appl Numer Methods* 1988;4:709-712
17. Hinton E, Campbell JS. Local and global smoothing of discontinuous finite element functions using a least squares method. *Int J Numer Method Eng* 1974;8:461-480
18. Raphael O, Hervé R. *Clinical applications of rapid prototyping models in cranio-maxillofacial surgery*. In: Hoque M, ed. *Advanced Applications of rapid prototyping technology in modern engineering*. Rijeka, Croatia: InTech, 2011
19. Mankovich NJ, Samson D, Pratt W, Lew D, Beumer J 3rd. Surgical planning using three-dimensional imaging and computer modeling. *Otolaryngol Clin North Am* 1994;27:875-889
20. Choi JY, Choi JH, Kim NK, Kim Y, Lee JK, Kim MK, et al. Analysis of errors in medical rapid prototyping models. *Int J Oral Maxillofac Surg* 2002;31:23-32
21. Chang PS, Parker TH, Patrick CW Jr, Miller MJ. The accuracy of stereolithography in planning craniofacial bone replacement. *J Craniofac Surg* 2003;14:164-170
22. Schicho K, Figl M, Seemann R, Ewers R, Lambrecht JT, Wagner A, et al. Accuracy of treatment planning based on stereolithography in computer assisted surgery. *Med Phys* 2006;33:3408-3417
23. Ibrahim D, Broilo TL, Heitz C, de Oliveira MG, de Oliveira HW, Nobre SM, et al. Dimensional error of selective laser sintering, three-dimensional printing and PolyJet models in the reproduction of mandibular anatomy. *J Craniomaxillofac Surg* 2009;37:167-173
24. Silva DN, Gerhardt de Oliveira M, Meurer E, Meurer MI, Lopes da Silva JV, Santa-Bárbara A. Dimensional error in selective laser sintering and 3D-printing of models for craniomaxillary anatomy reconstruction. *J Craniomaxillofac Surg* 2008;36:443-449
25. Shellabear M, Nyrhilä O. DMLS-Development history and state of the art. Proceedings of the 4th LANE; 2004 Sep 21-24; Erlangen, Germany. Bamberg: Meisenbach-Verlag, 2004
26. Khaing MW, Fuh JY, Lu L. Direct metal laser sintering for rapid tooling: processing and characterization of EOS parts. *J Mat Proc Tech* 2001;113:269-272
27. Ohtani T, Kusumoto N, Wakabayashi K, Yamada S, Nakamura T, Kumazawa Y, et al. Application of haptic device to implant

dentistry--accuracy verification of drilling into a pig bone. *Dent Mater J* 2009;28:75-81

28. Müller A, Krishnan KG, Uhl E, Mast G. The application of rapid prototyping techniques in cranial reconstruction and preoperative planning in neurosurgery. *J Craniofac Surg* 2003;14:899-914

29. Poukens J, Haex J, Riediger D. The use of rapid prototyping in the preoperative planning of distraction osteogenesis of the cranio-maxillofacial skeleton. *Comput Aided Surg* 2003;8:146-154

30. Wagner JD, Baack B, Brown GA, Kelly J. Rapid 3-dimensional prototyping for surgical repair of maxillofacial fractures: a technical note. *J Oral Maxillofac Surg* 2004;62:898-901

31. Faber J, Berto PM, Quaresma M. Rapid prototyping as a tool for diagnosis and treatment planning for maxillary canine impaction. *Am J Orthod Dentofacial Orthop* 2006;129:583-589

32. Mavili ME, Canter HI, Saglam-Aydinatay B, Kamaci S, Kocadereli I. Use of three-dimensional medical modeling methods for precise planning of orthognathic surgery. *J Craniofac Surg* 2007;18:740-747

33. D'Urso PS, Earwaker WJ, Barker TM, Redmond MJ, Thompson RG, Effeney DJ, et al. Custom cranioplasty using stereolithography and acrylic. *Br J Plast Surg* 2000;53:200-204

34. Paiva WS, Amorim R, Bezerra DA, Masini M. Aplication of the stereolithography technique in complex spine surgery. *Arq Neuropsiquiatr* 2007;65:443-445

35. Armillotta A, Bonhoeffer P, Dubini G, Ferragina S, Migliavacca F, Sala G, et al. Use of rapid prototyping models in the planning of percutaneous pulmonary valved stent implantation. *Proc Inst Mech Eng H* 2007;221:407-416

36. Kim MS, Hansgen AR, Wink O, Quaife RA, Carroll JD. Rapid prototyping: a new tool in understanding and treating structural heart disease. *Circulation* 2008;117:2388-2394

37. Wurm G, Tomancok B, Pogady P, Holl K, Trenkler J. Cerebrovascular stereolithographic biomodeling for aneurysm surgery. Technical note. *J Neurosurg* 2004;100:139-145

38. Giesel FL, Hart AR, Hahn HK, Wignall E, Rengier F, Talanow R, et al. 3D reconstructions of the cerebral ventricles and volume quantification in children with brain malformations. *Acad Radiol* 2009;16:610-617

39. Guarino J, Tennyson S, McCain G, Bond L, Shea K, King H. Rapid prototyping technology for surgeries of the pediatric spine and pelvis: benefits analysis. *J Pediatr Orthop* 2007;27:955-960

40. Hurson C, Tansey A, O'Donnchadha B, Nicholson P, Rice J, McElwain J. Rapid prototyping in the assessment, classification and preoperative planning of acetabular fractures. *Injury* 2007;38:1158-1162

41. Hiramatsu H, Yamaguchi H, Nimi S, Ono H. [Rapid prototyping of the larynx for laryngeal frame work surgery]. *Nihon Jibiinkoka Gakkai Kaiho* 2004;107:949-955

42. Mahmood F, Owais K, Taylor C, Montealegre-Gallegos M, Manning W, Matyal R, et al. Three-dimensional printing of mitral valve using echocardiographic data. *JACC Cardiovasc Imaging* 2015;8:227-229

43. Yang DH, Kang JW, Kim N, Song JK, Lee JW, Lim TH. Myocardial 3-dimensional printing for septal myectomy guidance in a patient with obstructive hypertrophic cardiomyopathy. *Circulation* 2015;132:300-301

44. He J, Li D, Lu B, Wang Z, Tao Z. Custom fabrication of composite tibial hemi-knee joint combining CAD/CAE/CAM techniques. *Proc Inst Mech Eng H* 2006;220:823-830

45. Wang Z, Teng Y, Li D. [Fabrication of custom-made artificial semi-knee joint based on rapid prototyping technique: computer-assisted design and manufacturing]. *Zhongguo Xiu Fu Chong Jian Wai Ke Za Zhi* 2004;18:347-351

46. Lee MY, Chang CC, Ku YC. New layer-based imaging and rapid prototyping techniques for computer-aided design and manufacture of custom dental restoration. *J Med Eng Technol* 2008;32:83-90

47. Dai KR, Yan MN, Zhu ZA, Sun YH. Computer-aided custom-made hemipelvic prosthesis used in extensive pelvic lesions. *J Arthroplasty* 2007;22:981-986

48. Harrysson OL, Hosni YA, Nayfeh JF. Custom-designed orthopedic implants evaluated using finite element analysis of patient-specific computed tomography data: femoral-component case study. *BMC Musculoskelet Disord* 2007;8:91

49. Stevens B, Yang Y, Mohandas A, Stucker B, Nguyen KT. A review of materials, fabrication methods, and strategies used to enhance bone regeneration in engineered bone tissues. *J Biomed Mater Res B Appl Biomater* 2008;85:573-582

50. Peltola SM, Melchels FP, Grijpma DW, Kellomäki M. A review of rapid prototyping techniques for tissue engineering purposes. *Ann Med* 2008;40:268-280

51. Amerini A, Hatam N, Malasa M, Pott D, Tewarie L, Isfort P, et al. A personalized approach to interventional treatment of tricuspid regurgitation: experiences from an acute animal study. *Interact Cardiovasc Thorac Surg* 2014;19:414-418

52. Griffith LG, Naughton G. Tissue engineering--current challenges and expanding opportunities. *Science* 2002;295:1009-1014

53. Melchels FP, Domingos MA, Klein TJ, Malda J, Bartolo PJ, Hutmacher DW. Additive manufacturing of tissues and organs. *Prog Polym Sci* 2012;37:1079-1104

54. Huh D, Matthews BD, Mammoto A, Montoya-Zavala M, Hsin HY, Ingber DE. Reconstituting organ-level lung functions on a chip. *Science* 2010;328:1662-1668

55. Huh D, Hamilton GA, Ingber DE. From 3D cell culture to organs-on-chips. *Trends Cell Biol* 2011;21:745-754

56. Chung SK, Son YR, Shin SJ, Kim SK. Nasal airflow during respiratory cycle. *Am J Rhinol* 2006;20:379-384

57. Tek P, Chiganos TC, Mohammed JS, Eddington DT, Fall CP, Ifft P, et al. Rapid prototyping for neuroscience and neural engineering. *J Neurosci Methods* 2008;172:263-269

58. Canstein C, Cachot P, Faust A, Stalder AF, Bock J, Frydrychowicz A, et al. 3D MR flow analysis in realistic rapid-prototyping model systems of the thoracic aorta: comparison with in vivo data and computational fluid dynamics in identical vessel geometries. *Magn Reson Med* 2008;59:535-

546

59. Dhir V, Itoi T, Fockens P, Perez-Miranda M, Khashab MA, Seo DW, et al. Novel ex vivo model for hands-on teaching of and training in EUS-guided biliary drainage: creation of "Mumbai EUS" stereolithography/3D printing bile duct prototype (with videos). *Gastrointest Endosc* 2015;81:440-446

60. de Zélicourt D, Pekkan K, Kitajima H, Frakes D, Yoganathan AP. Single-step stereolithography of complex anatomical models for optical flow measurements. *J Biomech Eng* 2005;127:204-207

61. Giesel FL, Mehndiratta A, von Tengg-Kobligk H, Schaeffer A, Teh K, Hoffman EA, et al. Rapid prototyping raw models on the basis of high resolution computed tomography lung data for respiratory flow dynamics. *Acad Radiol* 2009;16:495-498

62. Sulaiman A, Boussel L, Taconnet F, Serfaty JM, Alsaid H, Attia C, et al. In vitro non-rigid life-size model of aortic arch aneurysm for endovascular prosthesis assessment. *Eur J Cardiothorac Surg* 2008;33:53-57

63. Birjiniuk J, Ruddy JM, Iffrig E, Henry TS, Leshnower BG, Oshinski JN, et al. Development and testing of a silicone in vitro model of descending aortic dissection. *J Surg Res* 2015;198:502-507

64. Veeraswamy RK, Birjiniuk J, Ruddy JM, Timmins L, Oshinski JN, Ku DN. PC42. Phase-contrast magnetic resonance imaging reveals novel fluid dynamics in a patient-derived silicone model of descending thoracic aortic dissection. *J Vasc Surg* 2015;61:128S-129S

65. Kim BJ, Kwon SU. Perforator infarction immediately distal to the stenosis of parental artery: is it hemodynamic? *J Stroke Cerebrovasc Dis* 2014;23:1991-1993

66. Suzuki M, Ogawa Y, Kawano A, Hagiwara A, Yamaguchi H, Ono H. Rapid prototyping of temporal bone for surgical training and medical education. *Acta Otolaryngol* 2004;124:400-402

67. Bruyère F, Leroux C, Brunereau L, Lermusiaux P. Rapid prototyping model for percutaneous nephrolithotomy training. *J Endourol* 2008;22:91-96

68. Kalejs M, von Segesser LK. Rapid prototyping of compliant human aortic roots for assessment of valved stents. *Interact Cardiovasc Thorac Surg* 2009;8:182-186

69. Waran V, Narayanan V, Karuppiah R, Owen SL, Aziz T. Utility of multimaterial 3D printers in creating models with pathological entities to enhance the training experience of neurosurgeons. *J Neurosurg* 2014;120:489-492

70. Narayanan V, Narayanan P, Rajagopalan R, Karuppiah R, Rahman ZA, Wormald PJ, et al. Endoscopic skull base training using 3D printed models with pre-existing pathology. *Eur Arch Otorhinolaryngol* 2015;272:753-757